

Identification of Dynamic Parameters for Flexible Rotor AMBs System Considering Residual Unbalances

Yuanping Xu*, Jin Zhou*, Chaowu Jin* and Longxiang Xu*

* College of Mechanical and Electrical Engineering, Nanjing University of Aeronautics and Astronautics

29 Yudao Street, Nanjing, 210016, China

E-mail: ypxu@nuaa.edu.cn, zhj@nuaa.edu.cn, jinchaowu@nuaa.edu.cn, fqp@nuaa.edu.cn

Abstract

Active magnetic bearings (AMBs) support rotors using electromagnetic force rather than mechanical force. It is necessary to accurately identify AMBs force coefficients (equivalent stiffness and damping) since they play a key role in the rotordynamic analysis. The identification is usually performed by analyzing the unbalance response; however, the unknown residual unbalances will decrease the identification accuracy and rigid rotor model is only available when the rotating speed is far below the bending critical speed. To address the above issues, this paper proposes an identification algorithm to estimate the stiffness and damping parameters of a flexible rotor AMBs system using two independent unbalance response data. The proposed algorithm is employed for experimental identification for a flexible rotor AMBs system ranging from 3,000 rpm (50 Hz) to 30,000 rpm (500 Hz).

Keywords : AMBs, Flexible Rotor, Stiffness and Damping, Identification, Residual Unbalances

1. Introduction

Active magnetic bearings generate forces through magnetic fields rather than mechanical forces as in lubricated fluid films or contact of rolling element bearings; therefore, the special advantage of AMBs is that there is no contact between bearings and rotor, and this permits operation with no lubrication, no mechanical wear, long life, lower costs and high attainable rotating speed (Schweitzer and Maslen, 2009). Another attractive advantage of AMBs is that the dynamic magnetic force parameters, equivalent stiffness and damping, are closely related to the feedback controller parameters, which can be changed easily (Lim and Cheng, 2007), such that the rotordynamics can be controlled and changed actively through the bearings.

For traditional mechanical bearings, it is vital to accurately obtain the dynamic parameters since these coefficients are the foundation for the rotordynamics analysis. Different from the mechanical bearings, for the AMBs, the identification usually could be classified into the following two aspects: (1) identify the force/displacement factor and the force/current factor (Kim and Lee, 1999; Tiwari and Talatam, 2015; Tiwari and Chougale, 2014; Fang, et al., 2014; Tang, et al., 2014); (2) identify the equivalent stiffness coefficient and damping coefficient (Lim and Cheng, 2007; Humphris, et al., 1986; Williams, et al., 1990; Lim, et al., 2011; Zhou, et al., 2016). Both identifications play an important role for the rotor AMBs system. Specifically, the force/displacement factor and the force/current factor is the key in any current controlled active magnetic bearing controller design process since they reflect the property of magnetic force without controlling; the equivalent stiffness and damping coefficients are the foundation for the rotor dynamics analysis since the controller effects are considered in this condition. This paper is trying to identify the equivalent stiffness and damping coefficients for a flexible rotor AMBs system.

Research has been carried out on the estimation of equivalent stiffness and damping parameters of AMBs, but most of these works have been done for a rigid rotor model at no rotating condition. The identification method using unbalance excitation and the corresponding unbalance response has been adopted in mechanical bearings (Santiago and San, 2007a, 2007b), however few works have been reported on its application for AMBs. The disadvantage of this method is that the existence of residual unbalance on the rotor could bring error in the unbalance excitation force calculation since the residual unbalance distribution is unknown and may change during operation for a flexible rotor.

Perfect balancing is very costly and sometimes even impossible. Thus, a certain amount of residual unbalance will always occur. In the present work, an algorithm is proposed to estimate the equivalent stiffness and damping parameters considering the residual unbalances in a flexible rotor that is fully levitated by AMBs. The proposed method is applied to our test rig to identify the AMBs stiffness and damping coefficients ranging from 3,000 rpm (50 Hz) to 30,000 rpm (500 Hz).

The remainder of the paper is organized as follows. Section 2 describes the rotor AMBs test rig employed in this paper and the mathematical modeling. Section 3 presents the identification method based on rotor unbalance responses. Section 4 describes the unbalance responses and experimental results. Conclusions are drawn in Section 5.

2. Test rig description and flexible rotor modeling

The experimental test rig for this study is designed and built as a research platform, which is pictured in Fig. 1. The rotor is supported by two radial and two thrust AMBs and is 0.468 m long and weighs around 2.4 kg. Table 1 summarizes the physical properties of radial AMBs employed in the test rig.

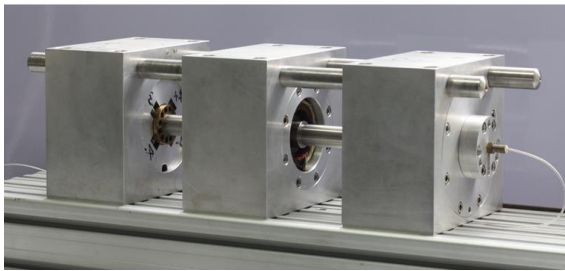


Fig. 1. An overview of the rotor AMBs test rig.

Nelson-Timoshenko beam (Nelson, 1980) finite element matrices are adopted to model the rotor according to the geometrical and mass information. The assembled parts such as lamination stacks are modeled as lumped mass onto the corresponding nodes. Ignoring two DOFs in axial direction, each node contains 2 translational and 2 rotational DOFs. After assembling the governing equations for all the elements and incorporating the boundary conditions, the linearized equations of motion for the shaft can be expressed as

$$\mathbf{M}_R \ddot{q} + (\mathbf{C}_R + \Omega \mathbf{G}_R) \dot{q} + \mathbf{K}_R q = f(t), \quad (1)$$

where q and $f(t)$ are generalized displacement and generalized force vector in two radial directions; Ω is the rotation speed; \mathbf{M}_R , \mathbf{C}_R and \mathbf{K}_R represent square symmetric mass, damping and stiffness matrices, respectively; \mathbf{G}_R is the skew symmetric gyroscopic matrix. For the rotor of our test rig in this study, its theoretical free-free undamped mode shapes is shown in Fig. 2. The first bending critical speed is around 480 Hz (28,800 rpm).

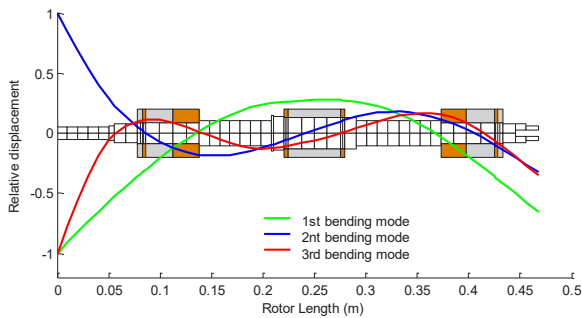


Fig. 2. Theoretical mode shapes of free-free rotor.

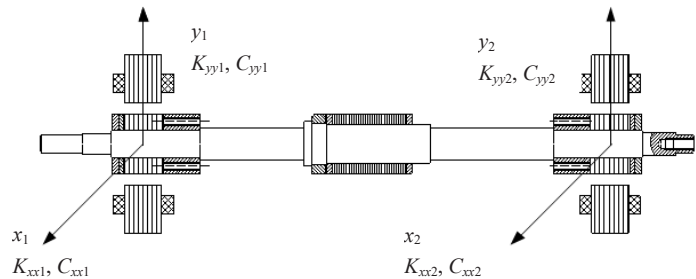


Fig. 3. Rotor coordinate system.

Fig. 3 illustrates the rotor's coordinate system, namely the four axes that are used in stiffness and damping coefficients identification. The AMBs force coefficients are modeled as stiffness \mathbf{K}_B and damping \mathbf{C}_B . Considering the residual unbalances effects on the rotor, the equations of motion of the rotor AMBs system can be written as follow,

$$\mathbf{M}_R \ddot{q} + (\mathbf{C}_R + \mathbf{C}_B + \Omega \mathbf{G}_R) \dot{q} + (\mathbf{K}_R + \mathbf{K}_B) q = f_{unb} + f_{res} \quad (2)$$

where q is generalized displacement vector in two radical directions; f_{unb} is the unbalance force generated by the known unbalanced mass screwed on the rotor; f_{res} is the residual unbalances force generated by the residual mass from the rotor, which can be written as follow:

$$q = [q_1 \quad \dots \quad q_{B1} \quad \dots \quad q_{B2} \quad \dots \quad q_N]^T;$$

$$q_i = [x_i \quad y_i \quad \beta_{xi} \quad \beta_{yi}], \quad i=1 \dots N$$

$$f_u = [0 \quad \dots \quad f_u \quad \dots \quad 0]^T;$$

$$\begin{aligned} & \mathbf{f}_{res} \\ & = [\mathbf{f}_{r1} \quad \mathbf{f}_{r2} \quad \dots \quad \mathbf{f}_{rN-1} \quad \mathbf{f}_{rN}] \end{aligned} \quad (3)$$

where q_{B1} and q_{B2} represent the displacements at two AMBs; x_i and y_i represent translations in the x and y directions; β_{xi} and β_{yi} are the angular displacements about the y and x axes, respectively; f_{ri} is the unknown residual unbalances force generated from rotor. f_u is the unbalance excitation force generated by known unbalance mass screwed on the rotor, which can be written as:

$$f_u = \begin{pmatrix} f_x \\ f_y \\ 0 \\ 0 \end{pmatrix} = m_u r \omega^2 \begin{pmatrix} \cos(\omega t + \varphi) \\ \sin(\omega t + \varphi) \\ 0 \\ 0 \end{pmatrix} = m_u r \omega^2 \begin{pmatrix} e^{i(\omega t + \varphi)} \\ -ie^{i(\omega t + \varphi)} \\ 0 \\ 0 \end{pmatrix} \quad (4)$$

where m_u is the unbalance mass; r is the radius between the unbalance location and the axis of shaft. Note that the periodic forced excitation with frequency ω caused by rotor unbalance is synchronous with rotating speed, i.e. $\omega = \Omega$. In general, $f_{unb} = \mathbf{F}_{unb} e^{i\omega t}$ and $f_{res} = \mathbf{F}_{res} e^{i\omega t}$, so the unbalance response possesses the same frequency as the excitation, i.e. $q = \mathbf{q} e^{i\omega t}$. Therefore, (2) can be written as the following algebraic form:

$$[(\mathbf{K}_R + \mathbf{K}_B - \mathbf{M}_R \omega^2) + i\omega(\mathbf{C}_R + \mathbf{C}_B + \Omega \mathbf{G}_R)] \mathbf{q} = \mathbf{F}_{unb} + \mathbf{F}_{res}, \quad (5)$$

where

$$\mathbf{K}_B = \begin{bmatrix} 0 & \dots & \dots & \dots & \dots \\ \dots & \mathbf{K}_{b1} & \dots & \dots & \dots \\ \dots & \dots & 0 & \dots & \dots \\ \dots & \dots & \dots & \mathbf{K}_{b2} & \dots \\ \dots & \dots & \dots & \dots & 0 \end{bmatrix}; \quad \mathbf{C}_B = \begin{bmatrix} 0 & \dots & \dots & \dots & \dots \\ \dots & \mathbf{C}_{b1} & \dots & \dots & \dots \\ \dots & \dots & 0 & \dots & \dots \\ \dots & \dots & \dots & \mathbf{C}_{b2} & \dots \\ \dots & \dots & \dots & \dots & 0 \end{bmatrix}. \quad (6)$$

The AMBs stiffness and damping matrices incorporate the following (yet unknown) coefficients:

$$\mathbf{K}_{bi} = \begin{bmatrix} K_{xxi} & 0 \\ 0 & K_{yyi} \end{bmatrix}_i; \quad \mathbf{C}_{bi} = \begin{bmatrix} C_{xxi} & 0 \\ 0 & C_{yyi} \end{bmatrix}_i, \quad i=1,2. \quad (7)$$

3. Identification algorithm considering the residual unbalances effects

The identification algorithm for the AMBs stiffness and damping coefficients is based on the measurement of rotor unbalance response caused by known unbalance mass screwed on the rotor. However most of these identification algorithms are proposed for a rigid rotor model and the unknown residual unbalance is not considered, which is only available when the running speed is far below the bending critical speed. In this paper, we proposed a new identification algorithm, which could eliminate the residual unbalance negative influence for a flexible AMBs rotor system.

In (2), the \mathbf{F}_{unb} could be calculated easily from the known unbalance mass screwed on the rotor and the corresponding rotating speed, but the residual unbalance force \mathbf{F}_{res} is difficult to acquire. However, we can eliminate the residual unbalance disadvantages from two groups of independent unbalance response data. In group 1#, the rotor operates without adding known unbalance mass. In group 2#, the known unbalance mass is screwed on the rotor. Therefore, the algebraic form of (5) for each group can be written as

$$[(\mathbf{K}_R + \mathbf{K}_B - \mathbf{M}_R \omega^2) + i\omega(\mathbf{C}_R + \mathbf{C}_B + \Omega \mathbf{G}_R)] \mathbf{q}_1 = \mathbf{F}_{res}, \quad (8)$$

$$[(\mathbf{K}_R + \mathbf{K}_B - \mathbf{M}_R \omega^2) + i\omega(\mathbf{C}_R + \mathbf{C}_B + \Omega \mathbf{G}_R)]\mathbf{q}_2 = \mathbf{F}_{unb} + \mathbf{F}_{res} \quad (9)$$

where the \mathbf{q}_1 and \mathbf{q}_2 represent the unbalance response for each group. \mathbf{F}_{unb} is the known unbalance force screwed on the rotor. Note that residual unbalance force \mathbf{F}_{res} is equivalent in these two conditions since the residual unbalance mass is not changed. So, the residual unbalance effects can be removed by (9)-(8), which can be written as,

$$[(\mathbf{K}_R + \mathbf{K}_B - \mathbf{M}_R \omega^2) + i\omega(\mathbf{C}_R + \mathbf{C}_B + \Omega \mathbf{G}_R)]\mathbf{q}_m = \mathbf{F}_{unb} \quad (10)$$

where

$$\mathbf{q}_m = \mathbf{q}_2 - \mathbf{q}_1 \quad (11)$$

therefore, the transfer function between unbalance excitation and displacement (dynamic stiffness matrix) is

$$\mathbf{H} = [(\mathbf{K}_R + \mathbf{K}_B - \mathbf{M}_R \omega^2) + i\omega(\mathbf{C}_R + \mathbf{C}_B + \Omega \mathbf{G}_R)] \quad (12)$$

here, the dynamic rotor stiffness matrix \mathbf{H}_R and dynamic AMBs stiffness matrix \mathbf{H}_B can be defined as

$$\mathbf{H}_R = [(\mathbf{K}_R - \mathbf{M}_R \omega^2) + i\omega(\mathbf{C}_R + \Omega \mathbf{G}_R)]$$

$$\mathbf{H}_B = \mathbf{K}_B + i\omega \mathbf{C}_B. \quad (13)$$

Combining the dynamic rotor stiffness matrix and dynamic AMBs stiffness matrix together, the (10) can be written as below:

$$\mathbf{H}\mathbf{q}_m = (\mathbf{H}_R + \mathbf{H}_B)\mathbf{q}_m = \mathbf{F}_{unb}. \quad (14)$$

Define Z_{B1} and Z_{B2} are the transitional displacement vectors of AMBs supporter places, which is expressed by

$$Z_{B1} = [x_{B1} \quad y_{B1}]^T;$$

$$Z_{B2} = [x_{B2} \quad y_{B2}]^T \quad (15)$$

where $(x_B \quad y_B)$ are the measured synchronous rotor responses at AMBs places. In order to identify the unknown AMBs coefficients, the algebraic system of (14) is reordered by use of matrix operations to bring the supporting displacement vectors Z_{B1} and Z_{B2} into the upper rows,

$$\bar{\mathbf{H}}_R \begin{Bmatrix} Z_{B1} \\ Z_{B2} \\ Z_O \end{Bmatrix} + \bar{\mathbf{H}}_B \begin{Bmatrix} Z_{B1} \\ Z_{B2} \\ Z_O \end{Bmatrix} = \begin{Bmatrix} 0 \\ 0 \\ \bar{\mathbf{F}}_{unb} \end{Bmatrix} \quad (16)$$

where Z_O is other displacement vectors except Z_{B1} and Z_{B2} . The $\bar{\mathbf{H}}_R$ and $\bar{\mathbf{H}}_B$ are the reordered matrix for \mathbf{H}_R and \mathbf{H}_B , respectively.

In order to calculate conveniently, $\bar{\mathbf{H}}_R$ and $\bar{\mathbf{H}}_B$ are partitioned into sub matrices like below:

$$\bar{\mathbf{H}}_R = \begin{bmatrix} \mathbf{H}_{R11} & \mathbf{H}_{R12} & \mathbf{H}_{R13} \\ \mathbf{H}_{R21} & \mathbf{H}_{R22} & \mathbf{H}_{R23} \\ \mathbf{H}_{R31} & \mathbf{H}_{R32} & \mathbf{H}_{R33} \end{bmatrix}; \bar{\mathbf{H}}_B = \begin{bmatrix} \mathbf{H}_{B1} & 0 & 0 \\ 0 & \mathbf{H}_{B2} & 0 \\ 0 & 0 & 0 \end{bmatrix} \quad (17)$$

where \mathbf{H}_{B1} and \mathbf{H}_{B2} are the dynamic matrix for the two radical AMBs, which are written as

$$\mathbf{H}_{Bi} = \begin{bmatrix} K_{xxi} + i\Omega C_{xxi} & 0 \\ 0 & K_{yyi} + i\Omega C_{yyi} \end{bmatrix}, i=1,2 \quad (18)$$

such that Eq. (16) becomes:

$$\begin{bmatrix} \mathbf{H}_{R11} & \mathbf{H}_{R12} & \mathbf{H}_{R13} \\ \mathbf{H}_{R21} & \mathbf{H}_{R22} & \mathbf{H}_{R23} \\ \mathbf{H}_{R31} & \mathbf{H}_{R32} & \mathbf{H}_{R33} \end{bmatrix} \begin{Bmatrix} Z_{B1} \\ Z_{B2} \\ Z_O \end{Bmatrix} + \begin{bmatrix} \mathbf{H}_{B1} & 0 & 0 \\ 0 & \mathbf{H}_{B2} & 0 \\ 0 & 0 & 0 \end{bmatrix} \begin{Bmatrix} Z_{B1} \\ Z_{B2} \\ Z_O \end{Bmatrix} = \begin{Bmatrix} 0 \\ 0 \\ \bar{\mathbf{F}}_{unb} \end{Bmatrix}. \quad (19)$$

In (19), the motion of AMBs support places (Z_{B1}, Z_{B2}) and load vector $\bar{\mathbf{F}}_{unb}$ are obtained from measurements and known unbalance mass screwed on the rotor. So from the third row of this equation, Z_O can be expressed as

$$Z_O = \mathbf{H}_{R33}^{-1} \{ \bar{\mathbf{F}}_{unb} - \mathbf{H}_{R31} Z_{B1} - \mathbf{H}_{R32} Z_{B2} \} \quad (20)$$

from the first and second row of (19), we can obtain the follow equations,

$$\begin{aligned} \mathbf{H}_{R11}Z_{B1} + \mathbf{H}_{R12}Z_{B2} + \mathbf{H}_{R13}Z_O &= -\mathbf{H}_{B1}Z_{B1}; \\ \mathbf{H}_{R21}Z_{B1} + \mathbf{H}_{R22}Z_{B2} + \mathbf{H}_{R23}Z_O &= -\mathbf{H}_{B2}Z_{B2}. \end{aligned} \quad (21)$$

Here, we define the AMBs transmitted forces f_{B1} and f_{B2} , which can be written as,

$$\begin{aligned} f_{B1} &= -(\mathbf{H}_{R11}Z_{B1} + \mathbf{H}_{R12}Z_{B2} + \mathbf{H}_{R13}Z_O); \\ f_{B2} &= -(\mathbf{H}_{R21}Z_{B1} + \mathbf{H}_{R22}Z_{B2} + \mathbf{H}_{R23}Z_O). \end{aligned} \quad (22)$$

Because Z_O can be obtained from (20), the f_{B1} and f_{B2} values can be calculated. So the AMBs support coefficients are determined by:

$$\begin{aligned} \mathbf{H}_{B1} &= \begin{bmatrix} K_{xx1} + i\Omega C_{xx1} & 0 \\ 0 & K_{yy1} + i\Omega C_{yy1} \end{bmatrix} = f_{B1}Z_{B1}^{-1}; \\ \mathbf{H}_{B2} &= \begin{bmatrix} K_{xx2} + i\Omega C_{xx2} & 0 \\ 0 & K_{yy2} + i\Omega C_{yy2} \end{bmatrix} = f_{B2}Z_{B2}^{-1}. \end{aligned} \quad (23)$$

4. Experimental Identification Results

The rotor unbalance response measurements are conducted ranging from 3,000 rpm (50 Hz) to 30,000 rpm (500 Hz). The unbalance response less than 3,000 rpm is not recorded since the unbalance displacement amplitude is small. Table 2 shows the unbalance mass distributions adopted in the experiment. Two unbalance masses are screwed on rotor at node 17 and node 43, respectively. The threaded holes space at 30° apart on the rotor, which is shown in Fig. 4. The measurement data is collected demonstrated in the following flow chart in Fig. 5.

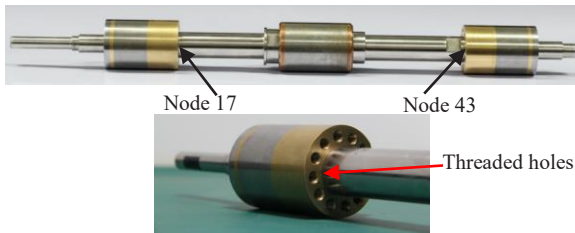


Fig. 4. The unbalance mass threaded holes.

Table 2
The known unbalance distributions on test rotor

Added place	Mass(g)	Radius(mm)	Phase(Deg.)
Node 17	0.98	15	0
Node 43	0.78	15	180

The rotating speed signal is measured by a non-contact fibre optical sensor, which is pictured in Fig. 6. The speed signal is treated as a reference signal for the measurement of phase for the entire displacements signals. During each run, the reference rotating signal is recorded at the same time with the displacement signals. The NI DAQ sampling module (NI 9215) is employed to convert the analog signal into digital signal. Then the digital signal is transmitted into the computer and stored by Labview program.

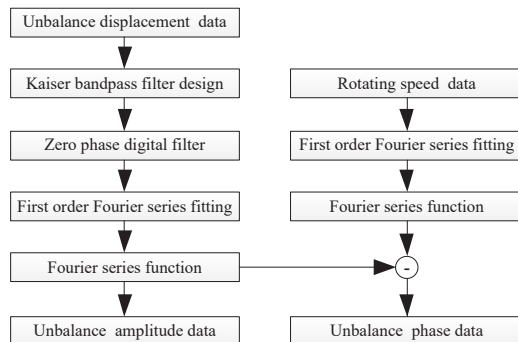


Fig. 5. The measurement data collection procedure.

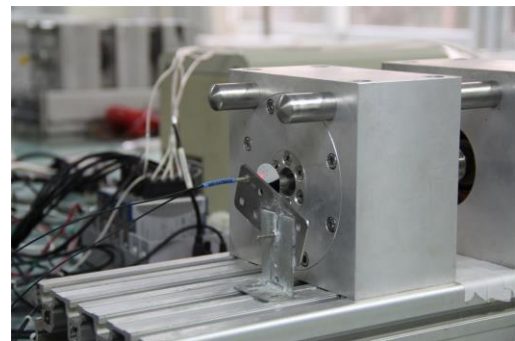


Fig. 6. Speed and reference signal measurement.

Since the stored time domain signal contains lots noise and we just care about those coincide with the rotating speed, we use the band-pass filter to process these signals. The Matlab function `kaiserord` is used to design n order band-pass filter for each speed signal. Conventional filter reduces noise in the signal, but delays the phase. By forward-backward

filtering, zero-phase lag filter reduces noise in the signal and preserves the phase at the same time it occurs in the original, which is common tool in off-line filter (Gustafsson, 1996) and employed to filter the time domain signals in this paper. Then use first order Fourier series based the least square method to fit the filtered signals, which could be written in the follow expression

$$y = a_0 + a_1 \cos(x\omega) + b_1 \sin(x\omega), \quad (24)$$

from the (24), the amplitude A and phase φ_d values under each rotating speed can be acquired though the parameters a_0, a_1, b_1, ω , which is written as

$$\begin{cases} A = \sqrt{a_1^2 + b_1^2} \\ \varphi_d = \arctan\left(\frac{a_1}{b_1}\right) \end{cases}. \quad (25)$$

Similarly, by performing the first order Fourier series fitting the reference rotating signals, the phase φ_r at each speed can be obtained. So, the real φ values for the entire displacements signals are written as

$$\varphi = \varphi_d - \varphi_r. \quad (26)$$

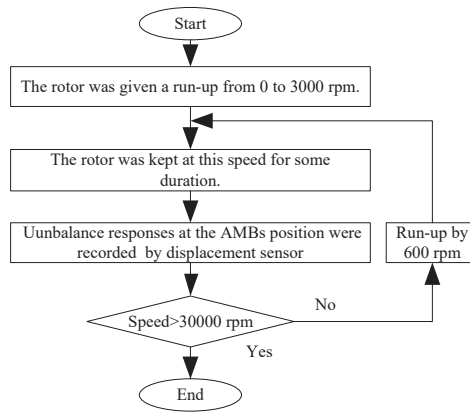


Fig. 7. Flowchart of test data process procedure.

Fig. 7 shows the unbalanced response test data processing procedure. Fig. 8 depicts the measured unbalance responses at bearings locations under rotating condition ranging from 50 Hz (3,000 rpm) to 500 Hz (30,000 rpm), in which only residual unbalance mass remains on the rotor. Fig. 8 shows the measured unbalance responses at AMBs locations resulting from the residual unbalance and the known unbalance masses screwed on the rotor.

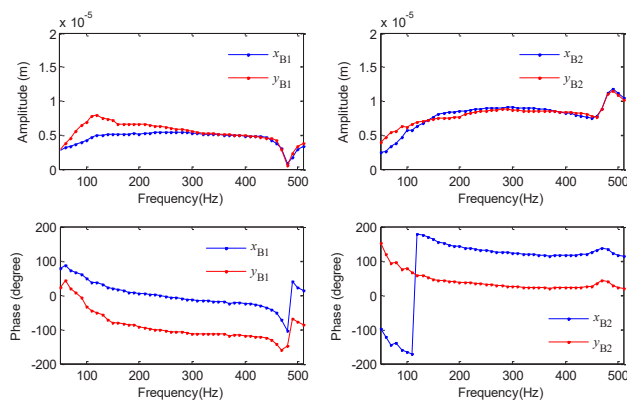


Fig. 7. Measured rotor unbalance responses (amplitude and phase) at AMBs locations, without known unbalance mass screwed.

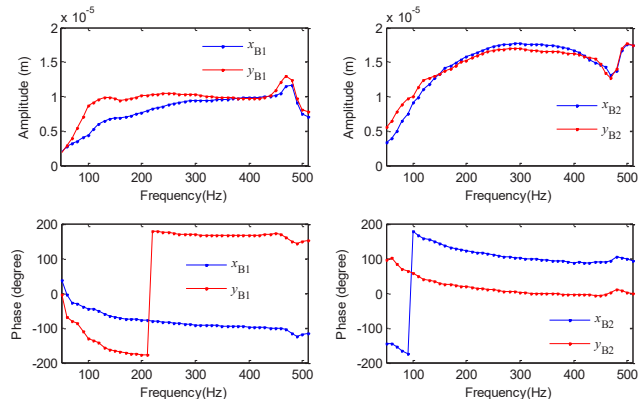


Fig. 8. Measured rotor unbalance responses (amplitude and phase) at AMBs locations, with known unbalance mass screwed.

Fig. 9 depicts the identified AMBs dynamic parameters, equivalent stiffness and damping, obtained from the two independent groups of rotor unbalance responses. It is seen that before the first bending critical speed (around 480 Hz), the equivalent stiffness and damping values increase steadily with the running speed. Since the control parameters for both x and y direction of each AMB are the same, the identified coefficients possess the same trend for the two orthogonal directions. However, there are still some small unclose agreement, which may be attributed to the small discrepancy in mechanical and electrical performance. The identified results fluctuate greater around the critical speed since the vibration near the circuitual speed becomes greater.

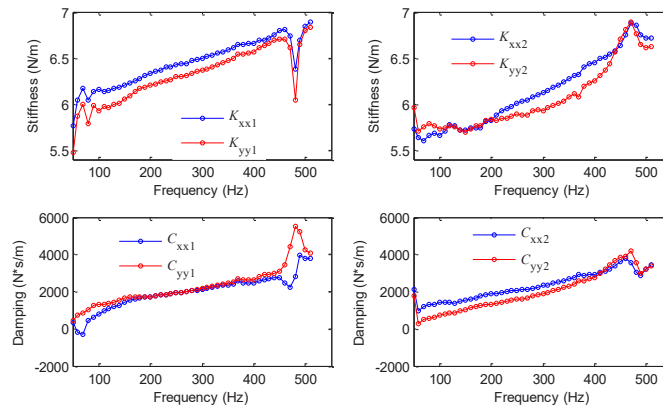


Fig. 9. Identified AMBs dynamic force coefficients versus rotor speed.

5. Conclusion and Discussion

This paper presented a AMBs dynamic force parameters identification algorithm for flexible rotor AMBs system. In order to improve the identification, the residual unbalance disadvantages are considered and eliminated from two independent unbalance tests. The proposed identification method is applied to experimental data from a AMBs rotor test rig and the identified results show that the stiffness and damping coefficients on both x and y axes vary along with the rotating speed.

Although the unbalance excitation is an easy and convenient excitation form for running rotor, some drawbacks cannot be neglected. For example unbalances beyond certain level may generate excessive unbalance force, which may break or damage the rotor system, especially for AMBs rotor system. In the experiment adopted in this paper, above 30,000 rpm (500 Hz) rotating speed is not performed due to the safety reason. Hence, acquiring the dynamic parameters by exciting the rotor using residual unbalance mass from the rotor itself or impulse response measurement may be a good choice. Current efforts are directed toward the identification methods mentioned above.

References

- Schweitzer G. and Maslen EH., Magnetic bearings: theory, design, and application to rotating machinery. Springer, Springer, NewYork, USA, 2009.
- Lim T.M. and Cheng S.B., Parameter estimation and statistical analysis on frequency-dependent active control forces, Mechanical systems and signal processing, vol. 21, No. 5 (2007), pp. 2112-2124.
- Kim S.J. and Lee C.W., On-line identification of current and position stiffnesses by LMS algorithm in active magnetic bearing system equipped with force transducers, Mechanical systems and signal processing, vol. 13, No. 5 (1999), pp. 681-690.
- Tiwari R. and Talatam V., Estimation of speed-dependent bearing dynamic parameters in rigid rotor systems levitated by electromagnetic bearings, Mechanism and Machine Theory, vol. 92, (2015), pp. 100-112.
- Tiwari R. and Chougale A., Identification of bearing dynamic parameters and unbalance states in a flexible rotor system fully levitated on active magnetic bearings, Mechatronics, vol. 24, No. 3 (2014), pp. 274-286.
- Fang J., Wang C. and Wen T., Design and Optimization of a Radial Hybrid Magnetic Bearing With Separate Poles for Magnetically Suspended Inertially Stabilized Platform, IEEE Transactions on Magnetics, vol. 50, No. 5 (2014), pp. 1-11.

- Tang J., Xiang B. and Zhang Y., Dynamic characteristics of the rotor in a magnetically suspended control moment gyroscope with active magnetic bearing and passive magnetic bearing, *ISA transactions*, vol. 53, No. 4 (2014), pp. 1357-1365.
- Humphris R.R., et al., Effect of control algorithms on magnetic journal bearing properties, *Journal of Engineering for Gas Turbines and Power*, vol. 108, No. 4 (1986), pp. 624-632.
- Williams R.D., Keith F. J. and Allaire P.E., Digital control of active magnetic bearings, *IEEE Transactions on Industrial Electronics*, vol. 37, No. 1 (1990), pp. 19-27.
- Lim T.M., et al., Design and parameter estimation of hybrid magnetic bearings for blood pump applications, *Mechanical Systems and Signal Processing*, vol. 23, No. 7 (2009), pp. 2352-2382.
- Tsai N.C., et al., Identification of rod dynamics under influence of Active Magnetic Bearing, *Mechatronics*, vol. 21, No. 6 (2011), pp. 1013-1024.
- Zhou J., et al., A rotor unbalance response based approach to the identification of the closed-loop stiffness and damping coefficients of active magnetic bearings, *Mechanical systems and signal processing*, vol. 66 (2016), pp. 665-678.
- Santiago De O.C. and San Andrés L., Field Methods for Identification of Bearing Support Parameters-Part I: Identification From Transient Rotor Dynamic Response due to Impacts, *Journal of Engineering for Gas Turbines and Power*, vol. 129, No. 1 (2007), pp. 205-212.
- Santiago De O.C., San Andrés L., Field methods for identification of bearing support parameters—part II: identification from rotor dynamic response due to imbalances, *Journal of Engineering for Gas Turbines and Power*, vol. 129, No.1 (2007), pp. 213-219.
- Nelson H.D., A finite rotating shaft element using Timoshenko beam theory, *Journal of mechanical design*, vol. 102, No. 4 (1980), pp. 793-803.
- Gustafsson F., Determining the initial states in forward-backward filtering, *IEEE Transactions on Signal Processing*, vol. 44 (1996), pp. 988-992.